Chapter 5

Electronic correlations as a function of the magnetic field

In Chapter 4 I have described the effects of electron-electron correlations in the system of N interacting electrons confined in a parabolic potential with no external fields. Let us now move on to discussing the properties of the system in the presence of a magnetic field.

Let us compare the orbital energy quantisation and characteristic interaction energies as a function of the magnetic field. As I have shown in Section 2.1, the single-particle energy spectrum in the presence of the field is characterised by two frequencies,

$$\omega_{\pm} = \sqrt{\omega_0^2 + \frac{1}{4}\omega_c^2} \pm \frac{1}{2}\omega_c, \tag{5.1}$$

where the cyclotron frequency ω_c increases linearly with the magnetic field. Thus, in large fields the frequency ω_+ approaches the cyclotron frequency, while the frequency ω_- approaches zero. Interactions, on the other hand, scale as

$$E_0 = \frac{\sqrt{\pi}}{\ell} = \sqrt{\pi}\left(\omega_0^2 + \frac{1}{4}\omega_c^2\right)^{1/4}, \tag{5.2}$$

i.e., they increase with the magnetic field. Thus, for sufficiently large ω_0, in low magnetic

field the single-particle orbital energy quantisation will dominate, while the regime of large magnetic fields is the regime of strong interactions.

5.1 Collapse of the $\nu = 2$ phase of the quantum Hall droplet

I start my presentation by summarising the most important points of the paper "Theory of spin-singlet filling factor $\nu = 2$ quantum Hall droplet", published by Andreas Wensauer, Marek Korkusiński, and Pawel Hawrylak in Physical Review B, vol. 67, page 035325 (2003). This publication is an integral part of this thesis and is appended to the presented material.

In this paper we discuss the stability of the $\nu = 2$ phase of the quantum Hall droplet composed of an even number of $2N$ electrons in a parabolic confinement and in the magnetic field. First let us explain what the $\nu = 2$ phase is by distributing the $2N$ electrons on the levels of the single-particle parabolic energy spectrum, presented in Figure 5.1 (a). In this Figure I show several single-particle orbitals $(0, m, \sigma)$ forming the lowest Landau level, and two orbitals $(1, 0, \sigma)$ belonging to the second Landau level (for discussion of Landau levels in parabolic confinement, see Section 2.1). The confinement energy of the quantum dot $\hbar\omega_0 = 6$ meV, and the Zeeman energy is artificially enhanced for better visibility. In finite magnetic fields there exists a ladder of low-energy states $(0, m, \sigma)$ whose energy is lower than that of the lowest-energy orbital $(1, 0, \sigma)$ of the second Landau level. Such a ladder is denoted in the Figure 5.1 (a) by the black bars. If one distributes the $2N$ electrons on these states, they will form spin-singlet pairs and occupy the single-particle orbitals with increasing quantum number m, as shown in Figure 5.1 (b) for eight electrons. This spin-singlet state of the electronic droplet is called the $\nu = 2$ phase in the terminology of the integer quantum Hall effect.

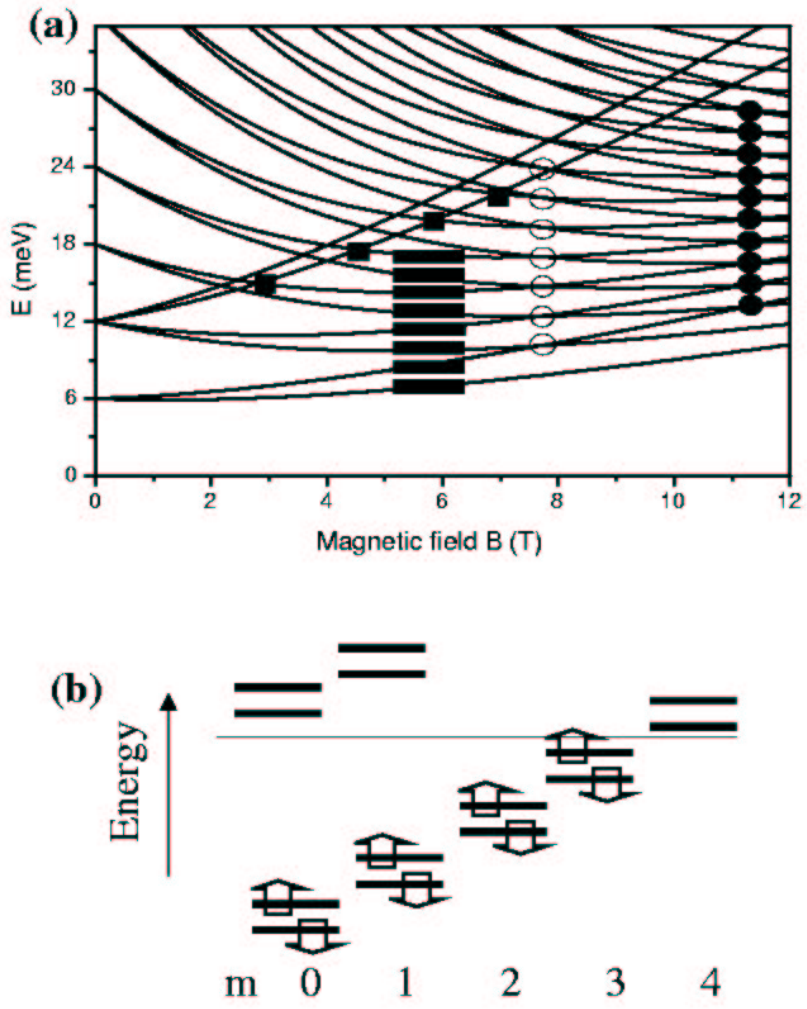

Figure 5.1: (a) Magnetic field evolution of the single-particle spectrum of the parabolic quantum dot (Zeeman energy artifically enhanced). Circles denote the edge spin flip of a droplet with even (empty) and odd (full) number of electrons; squares denote the centre spin flip. (b) Configuration of noninteracting electrons corresponding to the $\nu = 2$ phase

Let us now analyse the behaviour of this configuration as a function of the magnetic field. If the field is low enough, the states from the second Landau level may become lower in energy than the last occupied orbital on the lowest Landau level. These states are presented in Figure 5.1 (b) as empty levels with $m = 0$ and $m = 1$ above the Fermi energy, denoted by the black line. Due to the presence of the Zeeman energy, the electron on the last occupied orbital on the lowest Landau level $(0, 3)$ has spin up, while the lowest-energy state belonging to the second Landau level can contain the electron spin-down. Therefore, if the magnetic field is lowered sufficiently, a spin-flip transition will take place: the electron spin-up at the edge of the droplet will flip its spin and occupy the orbital $(1, 0, \downarrow)$ in the centre of the dot. These spin flips for different numbers of electrons are denoted in Figure 5.1 (a) with black squares.

If the magnetic field is increased, the separation between the consecutive orbitals of the lowest Landau level with the same spin (equal to $\hbar\omega_-$) decreases, and the Zeeman splitting increases linearly. For sufficiently high magnetic fields these two energies become equal: in Figure 5.1 (b) the lowest, empty, spin-down orbital with $m = 4$ becomes degenerate with the orbital with $m = 3$ occupied by the spin-up electron. This degeneracy will occur for the same magnetic field for all orbitals on the lowest Landau level; it is denoted with empty circles in Figure 5.1 (a). If the magnetic field is further increased, it becomes energetically favourable for the spin-up electron at the edge to flip its spin and move to the next orbital. Thus, the $\nu = 2$ phase is unstable against the centre spin-flip transition in low magnetic fields, and the edge spin-flip transition in high magnetic fields. Note that as more and more single-particle orbitals are populated with electrons, the range of magnetic fields in which the $\nu = 2$ phase is stable becomes narrower and narrower. It disappears completely for a critical number of electrons, for which the two spin-flip transitions occur at the same magnetic field (the last empty circle in Figure 5.1(a)). In this single-particle description the $\nu = 2$ phase diagram is thus finite, both as a function of the magnetic field and the number of electrons. However, due to the small value of

the Zeeman energy the predicted edge spin-flip transitions terminating the stability of the $\nu = 2$ phase would take place at magnetic fields of hundreds of Tesla while such transitions are observed experimentally for fields of order of a few Tesla. This discrepancy is due to my assumption of the absence of interactions. Our paper is devoted to understanding how the direct and exchange Coulomb interactions as well as electronic correlations modify the phase diagram of the system.

Let us start the analysis by considering the system in the lowest-Landau-level approximation (LLL). I write the wave function of the $\nu = 2$ phase as a product of two spin-polarised droplets:

$$|GS(2N)\rangle = \prod_{m=0}^{N-1} c^{+}_{0,m,\uparrow} \prod_{m=0}^{N-1} c^{+}_{0,m,\downarrow}|0\rangle. \tag{5.3}$$

The total energy of the $\nu = 2$ state is calculated as the expectation value $\langle GS(2N)|H|GS(2N)\rangle$ of the many-body Hamiltonian (3.2) analysed in Chapter 3. Now the particles are quasi-electrons dressed in interactions, and for further discussion it is convenient to define the selfenergy $\Sigma(n, m, \sigma)$, measuring the total interaction energy of the electron on orbital (n, m, σ) with all other electrons:

$$\Sigma(n, m, \sigma) = \sum_{m'=0}^{N-1} (2\langle nm, 0m'|V|0m', nm\rangle - \langle nm, 0m'|V|nm, 0m'\rangle). \tag{5.4}$$

Note that in this case this selfenergy does not depend on spin.

The centre and edge spin-flip configurations can now be expressed as excitations from the $\nu = 2$ state $|GS\rangle$. The wave function and corresponding energy of the centre configuration is

$$|C(2N)\rangle = c^{+}_{1,0,\downarrow} c_{0,(N-1),\uparrow}|GS(2N)\rangle; \tag{5.5}$$

$$\begin{aligned} E(C) &= E_{\nu=2} + \Omega_{+} - (N-1)\Omega_{-} - E_z \\ &+ \Sigma(1,0) - \Sigma(0,N-1) - \langle 0,(N-1);1,0|V|1,0;0,(N-1)\rangle. \end{aligned} \tag{5.6}$$

The energy $E(C)$ is calculated with respect to the energy $E_{\nu=2}$ of the $\nu = 2$ configuration. One quasielectron with spin up is taken off from the orbital $(0, N-1)$, and therefore the

appropriate orbital energy and selfenergy has to be subtracted from $E_{\nu=2}$. Then this quasielectron is put on the orbital $(1,0)$, and the orbital energy and selfenergy corresponding to this orbital has to be added. Further the spin of the particle is flipped, which results in the gain of Zeeman energy. The last term is the vertex correction, accounting for the attractive interaction of the quasielectron with the quasihole, which was created by removing the particle from the droplet.

As for the edge configuration, the corresponding wave function and energy are created in an analogous way:

$$|E(2N)\rangle = c^{+}_{0,N,\downarrow} c_{0,(N-1),\uparrow} |GS(2N)\rangle, \tag{5.7}$$

$$\begin{aligned} E(E) &= E_{\nu=2} + \Omega_{-} - E_z \\ &+ \Sigma(0,N) - \Sigma(0,N-1) - \langle 0,(N-1);0,N|V|0,N;0,(N-1)\rangle. \end{aligned} \tag{5.8}$$

Both these energies indicate that the spin-flip transitions take place as a result of the competition between the single-particle orbital energy and the interaction energy. For example, the interactions favour the edge spin-flip phase, because the edge spin-flip transition leads to (i) a redistribution of the last electron leading to a decrease of the direct repulsive Coulomb term, and (ii) an increase of the spin of the system, which leads to an increase of the exchange term, additionally lowering the energy. This is why in the case of the edge spin-flip transition the interactions play a role similar to that of the Zeeman energy in the noninteracting picture, but are strong enough to cause this transition in the magnetic fields of order of several Tesla. In the case of the centre spin-flip configuration the interplay of energies is more complicated: the spin is flipped, gaining the exchange energy, but the electron is put in the centre of the dot, which increases the Coulomb repulsion. The net result of this interplay drives the spin-flip transition to lower magnetic fields.

In order to be able to address the experimental spectra one needs to calculate the electrochemical potential of the $2N$-electron droplet: $\mu(2N) = E(2N+1) - E(2N)$. To

this end I also need to find the phase diagram of the $2N+1$-electron droplet. I do that by treating the extra particle as a quasielectron added to the state $|GS(2N)\rangle$ of the $2N$-electron droplet. This allows to calculate the energies of the system in a simple way, analogous to that described above.

For the $2N+1$-electron system I focus on a phase analogous to the $\nu = 2$, built out of the spin-singlet configuration for $2N$ particles as presented in Figure 5.1 (b), with the extra electron spin down on the next available orbital on the lowest Landau level (in this case, the orbital $(n, m) = (0, 4)$). As the magnetic field is lowered, this unpaired electron is transferred to the central orbital $(n, m) = (1, 0)$ of the second Landau level (without the spin flip). On the other hand, as the magnetic field is increased, the last edge electron with spin up (the electron on the orbital $(0, N)$; in Fig. 5.1 this electron occupies the orbital $(0, 3)$) is transferred over the unpaired electron to the orbital $(0, 5)$, and its spin is flipped. This transition leaves the system in a state with three unpaired spin-down electrons at the edge. These transitions occur at magnetic fields different than those corresponding to the centre and edge spin-flips of the $2N$-electron droplet. As a result, the electrochemical potential $\mu(2N)$ calculated as a function of the magnetic field is expected to exhibit a characteristic pattern of kinks. This pattern is indeed measured experimentally.

To improve the understanding of the role of direct and exchange Coulomb interactions, the $2N$-electron droplet is analysed using the spin- and space-restricted Hartree-Fock approach, as described in Section 3.2. For the $\nu = 2$ phase the variational Hartree-Fock wave function is written as

$$|GS(2N)\rangle = \prod_{\sigma} \prod_{m=0}^{N-1} (a^*_{0,m,\sigma} c^+_{0,m,\sigma} + a^*_{1,m+1,\sigma} c^+_{1,m+1,\sigma})|0\rangle, \tag{5.9}$$

i.e., the Hartree-Fock orbitals is constructed with definite angular momentum and spin out of the single-particle states from the two lowest Landau levels. The minimisation of the expectation value $\langle GS(2N)|H|GS(2N)\rangle$ with respect to the variational parameters a is written as an eigenvalue problem of the Hartree-Fock Hamiltonian within each angular

momentum and spin channel. The Hartree-Fock matrix is of order of 2×2, and is composed of the diagonal orbital energy terms, and both diagonal and offdiagonal self-consistent Hartree-Fock fields. A similar variational wave function is also constructed for the edge configuration $|E(2N)\rangle$ and the centre configuration $|C(2N)\rangle$, in the latter case allowing for the mixing of the second-Landau-level centre orbital $(1,0)$ with the orbital $(2,1)$ from the third Landau level. To calculate the phase diagram in this approximation, I compare the total energies calculated self-consistently for each of these three configurations as a function of the magnetic field and the number of electrons.

Finally, I attempt to account for the effects of electronic correlations. I do that using three different approaches: (i) single quasielectron-quasihole pair excitations from the Hartree-Fock $\nu = 2$ ground state, (ii) the exact diagonalisation, and (iii) the spin density functional theory.

As I have discussed in Section 3.3, the first approach involves calculating self-consistently the Hartree-Fock ground state $GS(2N)\rangle$ as expressed in Eq. (5.9), and use the optimal variational coefficients to construct the new creation and annihilation operators A^+, A, such that

$$A^+_{1l\sigma} = a^{*(1)}_{0l\sigma} c^+_{0l\sigma} + a^{*(1)}_{1,l+1,\sigma} c^+_{1,l+1,\sigma}, \tag{5.10}$$

$$A^+_{2l\sigma} = a^{*(2)}_{0l\sigma} c^+_{0l\sigma} + a^{*(2)}_{1,l+1,\sigma} c^+_{1,l+1,\sigma}. \tag{5.11}$$

The two sets of coefficients a are obtained in the eigenvalue problem of the Hartree-Fock Hamiltonian for each angular momentum and spin channel, even if the channel does not contain any electrons. Further the many-body Hamiltonian is rotated from the basis of operators c^+, c to the basis of operators A^+, A. The next step is to construct the basis set by distributing the quasiparticles on the Hartree-Fock orbitals. Here the basis is restricted to contain single quasielectron-quasihole pairs only, and therefore this basis set is composed of states of the type $A^+_{k,l+\delta l,\uparrow} A_{0l\downarrow} |\nu = 2\rangle_{HF}$. Note that in this way one only generates the electron-hole pair triplet excitations on the two lowest Landau levels. I am interested in the triplet states only, since both the centre and edge spin-flip configurations

are spin triplets. My pair excitations have a definite angular momentum $L_{\nu=2} + \delta l$, where $L_{\nu=2}$ is the angular momentum of the $\nu = 2$ state. Therefore I can group my pair excitations into subsets according to their angular momentum, and diagonalise the Hamiltonian matrix in each subset separately. Using this technique I am able to calculate the phase diagram of the electronic droplet containing even 30 electrons.

In the full exact diagonalisation approach I distribute my electrons on the single-particle orbitals, without rotating them into the Hartree-Fock basis. I generate all possible configurations of $2N$ electrons on two Landau levels, for all allowed values of total spin, and for total angular momenta from $L_{\nu=2} - 5$ to $L_{\nu=2} + 5$. Unfortunately now the total size of the basis, even after resolving the total angular momentum, total spin, and the projection of total spin, is so large that I am only able to analyse the magnetic field evolution of the system with 6 and 8 electrons.

The third approach to include correlations is the spin density functional theory in the local spin density approximation. Due to its effective single-particle character this approach allows to construct the phase diagram of the system for an arbitrary number of electrons. To remain consistent with the two other treatments in the calculation the Kohn-Sham orbitals are constructed only from the single-particle states belonging to the two lowest Landau levels.

In Figure 5.2 I present the phase diagrams of the $\nu = 2$ phase as a function of the number of electrons and magnetic field calculated using the five methods: the LLL approximation, the Hartree-Fock method on two Landau levels, the single quasielectron-quasihole pair excitations, the exact diagonalisation, and the SDFT. All phase diagrams were prepared using the GaAs material parameters assuming the same parabolic confinement energy $\hbar\omega_0 = 6$ meV. This is the central result of this work. In each diagram the $\nu = 2$ phase is stable only over a finite region of magnetic fields. Also, the four methods capable of treating large electron numbers reveal the existence of a critical number of electrons N_c, beyond which the $\nu = 2$ phase is not stable for any magnetic field. Differences

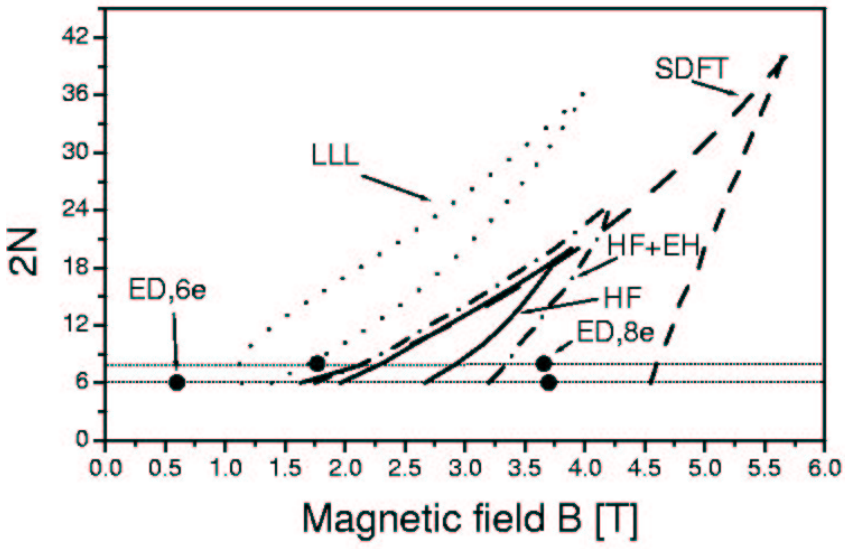

Figure 5.2: Phase diagrams obtained in the lowest Landau level approximation (dotted lines), using the Hartree-Fock approximation (solid lines), from single electron-hole pair excitation spectre (dot-dashed lines), using the SDFT approach (dashed lines), and from exact diagonalisation study (full circles)

between the phase diagrams lie only in positions of phase boundaries.

The LLL approximation predicts the occurrence of both spin-flip transitions at magnetic fields lower than those obtained with the other methods. This can be understood considering the fact that the spin flips are driven by interactions. In the LLL method the interactions were particularly strong, since the Hilbert space for each phase consisted of only one configuration. Other methods involved either self-consistent renormalisation of electronic orbitals (Hartree-Fock and SDFT) or writing the total wave function as a linear combination of many Slater determinants (single-pair excitations and exact diagonalisation). As a result, the electrons were allowed to redistribute in order to lower their repulsive Coulomb energy. This shifted the spin-flip transitions to larger magnetic fields.

Let us now compare the result of the Hartree-Fock method, accounting for the Coulomb direct and exchange interactions only, to that of the single-pair excitation approach, which partially includes the effects of correlations as well. The low-field phase boundary (i.e., the centre spin-flip) in both approaches is established by considering only one configuration, since in the pair excitation approach only one quasielectron-quasihole pair could be generated in the subspace of the centre spin-flip configuration. That is why the low-field boundaries predicted by each method almost coincide. On the other hand, the edge spin-flip state calculated in the pair excitation approach is correlated with the configurations involving occupation of the second Landau level, while in the Hartree-Fock theory it is approximated again by one configuration only. The phase boundaries predicted by these two approaches do not coincide; inclusion of correlations leads to an increase in stability range of the $\nu = 2$ phase. This is confirmed by the results of exact diagonalisation for 6 and 8 electrons, and SDFT for up to 42 electrons. Note that the SDFT calculation predicts a broader stability range of the spin-singlet phase towards higher magnetic fields than that obtained by exact diagonalisation. This is due to a slight overestimation of exchange effects in the SDFT procedure with the variational space reduced to two Landau levels. The regions of stability of the $\nu = 2$ phase obtained with the two approaches are much

larger than those predicted by the Hartree-Fock theory, both in magnetic fields (SDFT and exact diagonalisation) and in electron numbers (SDFT). Thus, electronic correlations counteract the exchange, and this is due to the fact that the exchange effects lower only the energy of the spin-polarised states, while correlation effects provide a mechanism to decrease the ground-state energies for the spin-singlet configurations as well.

In experiments the phase diagram is mapped out by analysing the addition spectrum obtained by measuring the electrochemical potential $\mu(2N) = E(2N+1) - E(2N)$. I have briefly presented this experimental procedure in Section 1.4. Such experiment is clearly sensitive both to the initial state of the N-electron droplet and the final state of the $N+1$-electron droplet. As I have already discussed, the spin-flip transitions manifest themselves in the addition spectra as series of kinks, and for low electron number it is possible to find the kinks corresponding to the centre spin-flip and the edge spin-flip transitions. However, for electron numbers larger than the critical number N_c the $\nu = 2$ phase is no longer stable. In this regime the centre-edge transition involves transfer of the spin-down electron from the centre orbital on the second Landau level directly to the first unoccupied orbital at the edge of the droplet (without spin flip). The experimental signature of this transition is similar to the transition from the $\nu = 2$ phase to the edge configuration for lower electron numbers, and the high-electron-number kinks appear as a continuation of the line of $\nu = 2$-edge transitions. Therefore, the collapse of the $\nu = 2$ phase is not revealed in the positions of the addition peaks. However, various alignments of stability regions can be probed by the spin-polarised tunnelling current due to the spin blockade phenomenon. In the experiment, the electrons tunnelling through the system are predominantly spin-down, and the current cannot flow if the spin of the final state of the $N + 1$-electron droplet is not equal to the spin of the initial state of the N-electron droplet plus one electronic spin down. Therefore, changes of the order of phases from centre-$\nu = 2$-edge (triplet-singlet-triplet) to centre-edge (triplet-triplet) are visible in the amplitude pattern of the addition peaks: the sequence of amplitudes of peaks as a function of the magnetic field for $2N < N_c$

is different than that for $2N > N_c$. The amplitude patterns of addition peaks is studied as a function of the parameters of the system (Zeeman energy and electron number). This amplitude reversal is almost not recovered if the approximation used overestimates exchange or correlations. In such cases the phase boundaries of the $\nu = 2$ and spin-triplet phases are shifted, which leads to their misalignment with respect to the phases of the $N + 1$-electron droplet. It is only when a proper balance between all interaction terms is found (e.g., by using an enhanced Zeeman energy in the SDFT calculations) that the reversal of amplitudes is obtained for a range of electron numbers.

5.2 Pairing of spin excitations in high magnetic fields

Up to now I have focused on the properties of the system of many electrons confined in a parabolic quantum dot in the region of stability of the $\nu = 2$ spin-singlet phase. In this Section I shall extend this discussion to higher magnetic fields. Research on this subject is presented in the paper "Pairing of spin excitations in lateral quantum dots", by Marek Korkusiński, Pawel Hawrylak, Mariusz Ciorga, Michel Pioro-Ladrière and Andrew S. Sachrajda, submitted for publication in Physical Review Letters. This publication is an integral part of this thesis and is appended to the presented material.

I shall present the analysis on the model system of eight electrons in a parabolic quantum dot. Let us first consider the magnetic-field evolution of the droplet within the lowest-Landau-level approximation. I have already shown that there exists a range of magnetic fields, in which the ground state of the system is the spin-singlet $\nu = 2$ state, shown schematically in Fig. 5.3 (a). As the magnetic field is increased, one sees a transition to the edge spin-triplet configuration, or the first spin-flip phase, shown in Fig. 5.3 (b). The value of the magnetic field corresponding to this transition is determined by the competition of the orbital energy, decreasing with the increase of the field, against Coulomb direct and exchange interactions, which increase with the field. If the magnetic

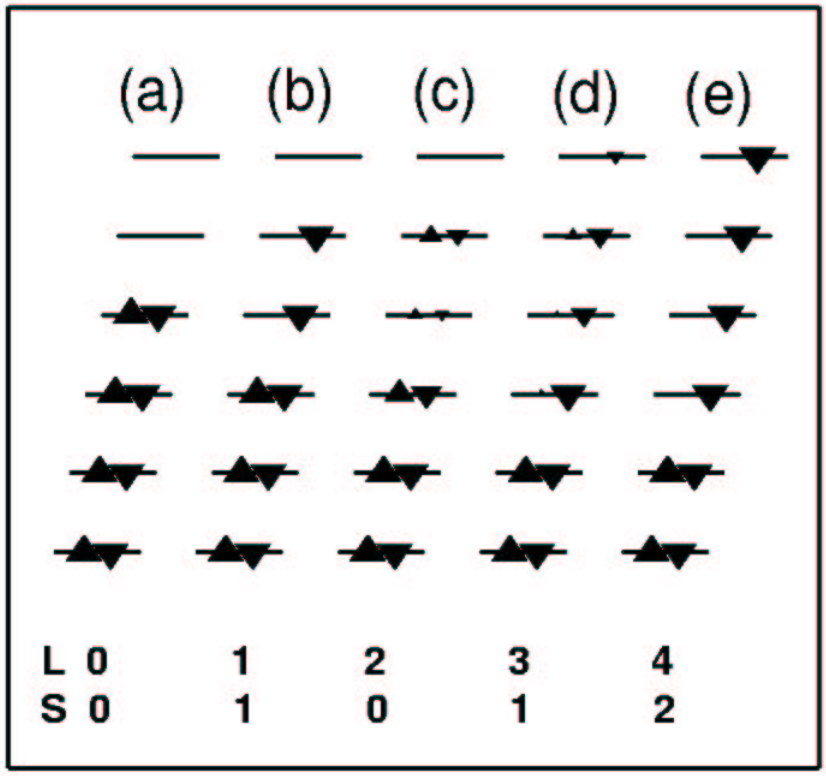

Figure 5.3: Charge distribution corresponding to the $\nu = 2$ phase (a), the first spin-flip configuration (b), the correlated biexciton (c), the internal spin-flip phase (d) and the second spin-flip configuration for an eight-electron parabolic dot

field is increased even further, one observes the second spin-flip transition - a transition from the configuration (b) to the configuration (e) in Fig. 5.3. As a result of this transition the droplet becomes even more spin-polarised (the second spin-flip phase has total spin 2), which increases the exchange energy, and the electrons are redistributed farther apart from one another, lowering the direct Coulomb repulsion. This sequence of spin flips continues until the dot becomes completely spin-polarised (this is the so-called maximum density droplet).

Note that the angular momentum of the first spin-flip configuration (b) is larger than that of the $\nu = 2$ phase by one: $L_{1SF} = L_{\nu=2} + 1$, and the angular momentum of the second spin-flip configuration (e) is $L_{2SF} = L_{\nu=2} + 4$. As can be seen, the sequence of spin flips predicted just by considering the direct and exchange interactions leaves the subspaces with angular momenta $L_{\nu=2} + 2$ and $L_{\nu=2} + 3$ unexplored.

I have analysed these unexplored subspaces within a simple exact-diagonalisation scheme, and found that by distributing the eight electrons on the single-particle orbitals of the lowest Landau level one can generate several electronic configurations with these angular momenta: there exist three singlet and two triplet configurations with $L = L_{\nu=2} + 2$ and five singlet and five triplet configurations with $L = L_{\nu=2} + 3$. The Hamiltonian matrix is diagonalised in these spin- and angular momentum-resolved basis sets. The resulting eigenstates are found have correlated character. In the subspace with $L = L_{\nu=2} + 2$ there are more singlets than triplets, and this correlation advantage causes the lowest singlet state to have lower energy than the lowest triplet. In the subspace with $L = L_{\nu=2} + 3$, on the other hand, the numbers of configurations with either spin are equal, and singlets do not have the correlation advantage. As a result, the lowest eigenstate of the Hamiltonian in this subspace is a spin triplet, since, being more spin-polarised, it has the exchange advantage over the singlets.

When the eigenenergies in the two subspaces are compared to the energies of the $\nu = 2$, first, and second spin-flip configurations, it turns out that for some regions of magnetic

fields the correlations lower the energies of the new states sufficiently for them to become ground states of the system.

Thus one obtains a new phase diagram, with two new phases occurring between the first and second spin-flip transitions. The distribution of the electronic charge of the first new correlated phase on the single-particle orbitals is shown in Fig. 5.3(c). It is a spin singlet, and it exhibits a spin-biexcitonic character, since its charge distribution clearly expresses a signature of a double hole below the $\nu = 2$ Fermi energy, and double electron above it. The second correlated phase, whose charge distribution is shown in Fig. 5.3(d), is a spin-triplet, and is predicted to become the ground state of the system just before the second spin flip. This phase can be described as a spin flip in the interior of the spin-biexciton phase. The last transition in the sequence is the second spin-flip, which terminates the correlated phases, and brings the system back to the weakly correlated ground state (e) in Fig. 5.3.

Note that the analysis accounting only for the direct and exchange interactions predicted a steplike increase of the total spin of the system: from the singlet $\nu = 2$ phase, through the triplet first spin-flip configuration, to the second spin-flip state with $S = 2$. Inclusion of correlations leads to the appearance of low-spin phases, having a correlation advantage over the high-spin configurations. As a result, the total spin exhibits an oscillatory character as a function of the magnetic field.

In Figure 5.4 I show the phase diagram of the even-electron system as a function of the magnetic field and the number of electrons. As I have shown earlier, the $\nu = 2$ phase has a finite stability region both in the magnetic field and in the number of electrons. For all the electron numbers for which $\nu = 2$ is stable I find a similar progression of phases as the magnetic field is increased: the $\nu = 2$ phase becomes unstable against the first spin-flip transition, which, in turn, is followed by the correlated biexciton, and finally the second spin-flip. The spin biexciton is stable even for very large electron numbers (of order of 30). In the phase diagram, I also find the correlated internal spin-flip phase, however it

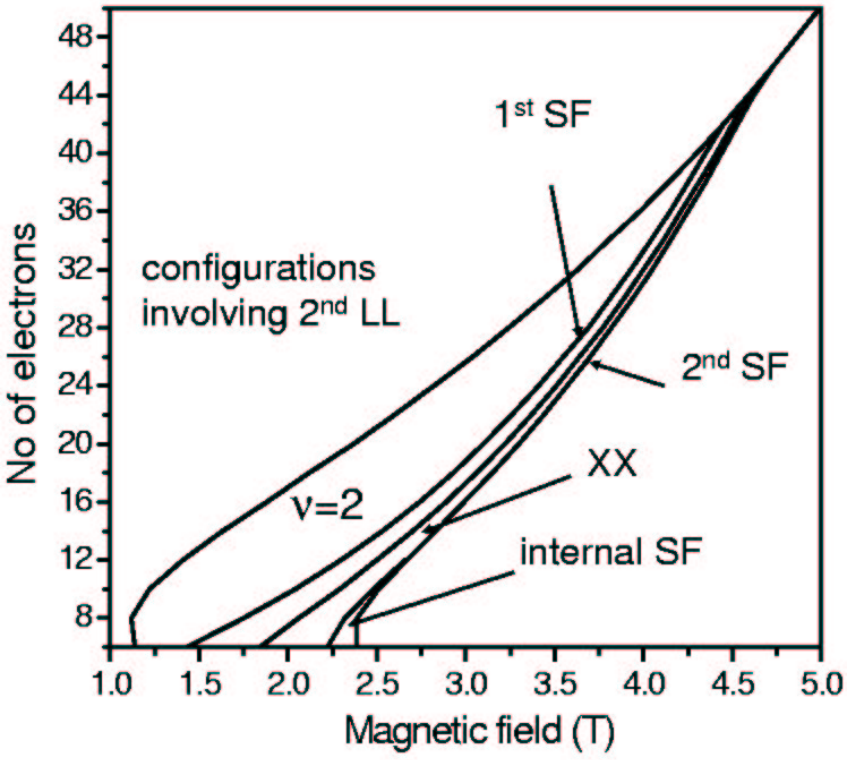

Figure 5.4: Phase diagram of the even-electron droplet as a function of the number of electrons and the magnetic field. In this calculation $\hbar\omega_0 = 6$ meV and the Zeeman energy $E_Z = 0$.

has a much smaller region of stability (this phase is no longer present for the number of electrons $N > 12$). Thus, both correlated phases should be visible in the experimental addition spectra measured for a QD with a sufficiently low number of electrons. The experimental evidence for the correlated phases is indeed found in the results of recent measurements of A.S. Sachrajda and his group at the NRC Institute for Microstructural Sciences. They have measured the addition spectra of the eighth electron into the seven-electron quantum dot in the high source-drain voltage mode. As discussed in Section 1.4, in this mode one can map not only the ground, but also the excited states of the system. The signatures of correlated phases in the vicinity of the second spin-flip are indeed found, and, to the best of my knowledge, this is the first experimental observation of correlated phases in a quantum dot with known and precisely controlled number of electrons. The correlated phases appear first as excited states, descend in energy with the increase of the magnetic field, and then some of them briefly become the ground states of the system.